Proteoglycan Research

WILEY

Proteoglycan Research

ORIGINAL RESEARCH OPEN ACCESS

Decorin Expressed From Herpes Simplex Virus Vector Improves Oncolytic Efficacy in Lung Adenocarcinoma Cells

Fanny Frejborg[1,2] | Jussi Palomäki[2] | Kiira Kalke[2] | Julius Orpana[2] | Oliver Koivisto[1] | Henrik Paavilainen[3] | Jessica M. Rosenholm[1] | Hongbo Zhang[1,4] | Veijo Hukkanen[2] | Hannu Järveläinen[2,5]

[1]Pharmaceutical Sciences Laboratory, Faculty of Science and Engineering, Åbo Akademi University, Turku, Finland | [2]Institute of Biomedicine, University of Turku, Turku, Finland | [3]Orion Corporation, Turku, Finland | [4]Turku Bioscience Centre, University of Turku and Åbo Akademi University, Turku, Finland | [5]Department of Internal Medicine, Satasairaala Central Hospital, The Wellbeing Services County of Satakunta, Pori, Finland

Correspondence: Fanny Frejborg (fanny.frejborg@abo.fi) | Hannu Järveläinen (hanjar@utu.fi)

Received: 8 November 2024 | **Revised:** 21 December 2024 | **Accepted:** 30 December 2024

Funding: F.F. would like to thank Åbo Akademi University Graduate School for personal funding in the form of PhD salary. The authors would further like to thank the Jane and Aatos Erkko foundation (#170046), Satasairaala Central Hospital, The Wellbeing Services County of Satakunta, Cancer Foundation of Southwestern Finland, State of Finland Research Fund (VTR), Research Council of Finland (project numbers #337531, #347897, #353146), Sigrid Jusélius foundation, The Paulo Foundation and Turku University foundation for funding this project. J.P. would like to thank The Finnish Cultural Foundation, South Ostrobothnia Regional Fund (grant number 10231545), Cancer Association of South-Western Finland (grant date 20211210) and Kauhajoki Cultural Foundation (grant date 20230421) for personal funding. K.K. and V.H. have also been supported by the research project 26004913 from Orion Pharma, Finland. This research is also aligned with the strategic research profiling area "Solutions for Health" at Åbo Akademi University (funded by the Research Council of Finland, #336355).

Keywords: decorin | herpes simplex vector | herpes simplex virus | lung cancer | lung carcinoma | oncolysis

ABSTRACT

Decorin (DCN) is a small extracellular proteoglycan with significant oncosuppressive activity. Lung adenocarcinoma is commonly devoid of DCN expression and is a leading cause of cancer mortality globally. As a proof-of-concept study for evaluating the oncosuppressive potential of DCN expression in lung adenocarcinoma cells, we constructed an oncolytic herpes simplex virus type 1 (HSV-1) vector, with a DCN transgene, using a transfection-infection method. Treatment of the lung adenocarcinoma cell line A549 with this novel DCN-expressing HSV-1 vector led to a significantly increased oncolysis of the cells compared to the effect of the parental or control marker virus. These results support the further development of a DCN-expressing oncolytic HSV-1 for evaluation in in vivo models for the treatment of lung adenocarcinoma, as well as other types of cancers with underexpressed DCN.

1 | Introduction

Decorin (DCN) is an extracellular matrix component that belongs to the small leucine-rich proteoglycan family. DCN is multifunctional, playing an important role in various biological processes, including wound healing and angiogenesis. Interestingly, DCN is often underexpressed in adenocarcinomas [1]. Lung cancer is one of the most frequently diagnosed cancers, of which adenocarcinoma is the most common, and is a leading cause of cancer mortality [1]. The 5-year survival rate of patients with lung adenocarcinoma varies, but is generally very poor despite modern treatments, amounting to 10–20% [2].

Abbreviations: BFP, blue fluorescent protein; CMV-IE, cytomegalovirus immediate early; DCN, decorin; DMEM, Dulbecco's modified Eagle medium; EF-1-alpha, elongation factor-1-alpha; EMEM, Eagle's minimum essential medium; FBS, fetal bovine serum; gD, glycoprotein D; GFP, green fluorescent protein; HSV, herpes simplex virus; MOI, multiplicity of infection.

Veijo Hukkanen and Hannu Järveläinen are shared senior authorship.

Mesenchymal cells, fibroblasts, keratinocytes, chondrocytes and smooth muscle cells, as well as stressed vascular endothelial cells, express DCN [3–7]. The 40 kDa glycoprotein core is leucine-rich and typically has one glycosaminoglycan side chain, either dermatan or chondroitin sulfate. The core protein consists of four distinct domains. These distinct domains endow DCN with its ability to bind to many matrix components and factors, including multiple growth factors such as tumor-, fibroblast-, and platelet-derived-growth factor [8–10]. DCN also binds to many receptors, including endothelial growth factor receptors [11]. DCN is known to bind to the d and e bands of type I collagen fibrils, from which DCN derives its name [12]. DCN also increases the stability of aggrecan in the articular cartilage and thus, regulates chondrocyte mechanotransduction and attenuates post-traumatic osteoarthritis [13–16].

Due to its multiple functions in the extracellular matrix, DCN is an important regulator of fibrillogenesis and thus, wound healing [17]. It has been shown that DCN defective animal models develop fibrosis after being wounded, and treatments based on DCN can improve wound healing and prevent the formation of fibrotic tissue [18–21]. DCN has also been shown to inhibit angiogenesis and functions in a tumor suppressive manner in many models [22, 23]. Thus, we hypothesized that induction of intratumoral DCN expression combined with oncolytic virotherapy could be efficacious against lung adenocarcinoma.

Efforts have been made to develop restoration of DCN expression in malignant cells [24–26]. A suitable vector with intrinsic oncolytic properties is the herpes simplex virus (HSV), whose oncolytic effect and safety has been proven in clinical settings with consequent market approval [27, 28]. Deleting the neurovirulence gene $\gamma_1$34.5 makes the virus conditionally replicative and weakens its virulence markedly [29]. The neurovirulence gene functions as an inhibitor of the host cell's defense mechanism, such as shutting off interferon signaling, inhibiting autophagy and reversing selective protein synthesis amongst many others [30–32]. By removing this gene, the virus can only replicate in cells that are defective in the aforementioned pathways, such as malignant cells with activated MEK that suppresses protein kinase R [33]. This replication is oncolytic and results in cell destruction that leads to the recruitment of the immune system [34]. We have in conjunction with a previous study successfully expressed marker genes with a recombinant HSV in the lungs of mice using intranasal administration, which would be a suitable way for delivery of the virus in vivo [35].

In this study, we constructed an HSV vector with a neurovirulence gene deletion and a DCN expression cassette and evaluated the role of DCN overexpression in the treatment of adenocarcinomas.

2 | Methods and Materials

2.1 | Cell Lines

BHK 21−13 s (hamster kidney cells, CCL-10, ATCC, Virginia, US) were maintained in Eagle's minimum essential medium (EMEM, Lonza, Basel, Switzerland) supplemented with 10% fetal bovine serum (FBS, Gibco, Thermo Fisher Scientific, Massachusetts, US) and gentamycin. Vero cells (African green monkey kidney cells, CCL-81, ATCC) and A549 cells (human lung adenocarcinoma, CCL-185, ATCC) were maintained in Dulbecco's modified eagle medium (DMEM, Thermo Fisher Scientific) 7% FBS, gentamycin and 5 mM GlutaMAX (Thermo Fisher Scientific).

2.2 | Recombinant Vector Construction

The shuttle plasmids used to construct H2252 and H2254 were purchased from VectorBuilder (Neu-Isenburg, Germany). Both plasmids contain a 45 bp 5' and 50 bp 3' H1052 homologous flank sequence of $\gamma_1$34.5 (Figure 1). The plasmid used for the construction of H2254, pH2254 (# VB210315-1088-mww, Supporting Information S1: Figure 1A), is a 6033 bp plasmid with a blue fluorescent protein (BFP) gene insert under a cytomegalovirus immediate early (CMV-IE) promoter with a SV40 poly (A) signal. The plasmid used for the construction of H2252, pH2252 (# VB221020-1473-syg, Supporting Information S1: Figure 1B), is an 8579 bp plasmid with a DCN insert under a CMV-IE promoter with a SV40 poly(A) signal and a BFP insert under an EF-1-alpha promoter with a bovine growth hormone poly(A) signal. The parental virus H1052, originally constructed using HSV bacterial artificial chromosome technology, described in Nygårdas et al. [37], is based on herpes simplex virus type 1 (HSV-1) (17+)Lox-Luc-$_{\Delta\gamma134.5}$-Zeo and has both $\gamma_1$34.5 copies deleted and an enhanced green fluorescent protein (GFP) transgene under an hCMV promoter in the left terminal copy of $\gamma_1$34.5 [38]. H1052 also has a luciferase cassette inserted between the genes U_L55 and U_L56 [38].

Plasmids were transfected into BHK 21-13 s cells grown in 96-well plates with lipofectamine 3000 (Thermo Fisher Scientific) using the manufacturer's protocol, with a modification of using double the recommended DNA amount per well. The cells were infected with H1052 at a multiplicity of infection (MOI) of 0.01 at 24 h post transfection. After 48 h post infection, the supernatant and the cells were collected. The purification of the virus was performed using a selection based on the fluorescence of the infected cells. The supernatant collected from the infected cells were diluted onto BHK 21−13 s cells, and when larger BFP positive plaques became visible, the cells were washed with PBS, the BFP positive plaques were marked and overlaid with low gelling temperature agarose. Next, the plaques were picked with a Pasteur pipette. The collected cells were suspended in 1:1 in 9% milk and EMEM supplemented with 7% FBS and gentamycin, and freeze thawed and sonicated. The process was repeated for two more passages after the plaques were GFP negative. In total, the H2252 was purified for 11 rounds and H2254 for 7 rounds. H2254 has EGFP replaced with BFP and H2252 has EGFP replaced with DCN under an hCMV promoter and with BFP under an EF1-α promoter. The vectors are illustrated in Figure 1A.

The viral stocks were cultured from the purified BFP positive/GFP negative plaques. Briefly, T175 flasks were seeded with Vero cells, and when 80−90% confluent was infected with the collected plaque. When the cells reached full cytopathic effect, they were scraped into the supernatant and pelleted. The pellet was resuspended in 9% milk, freeze thawed and sonicated. The

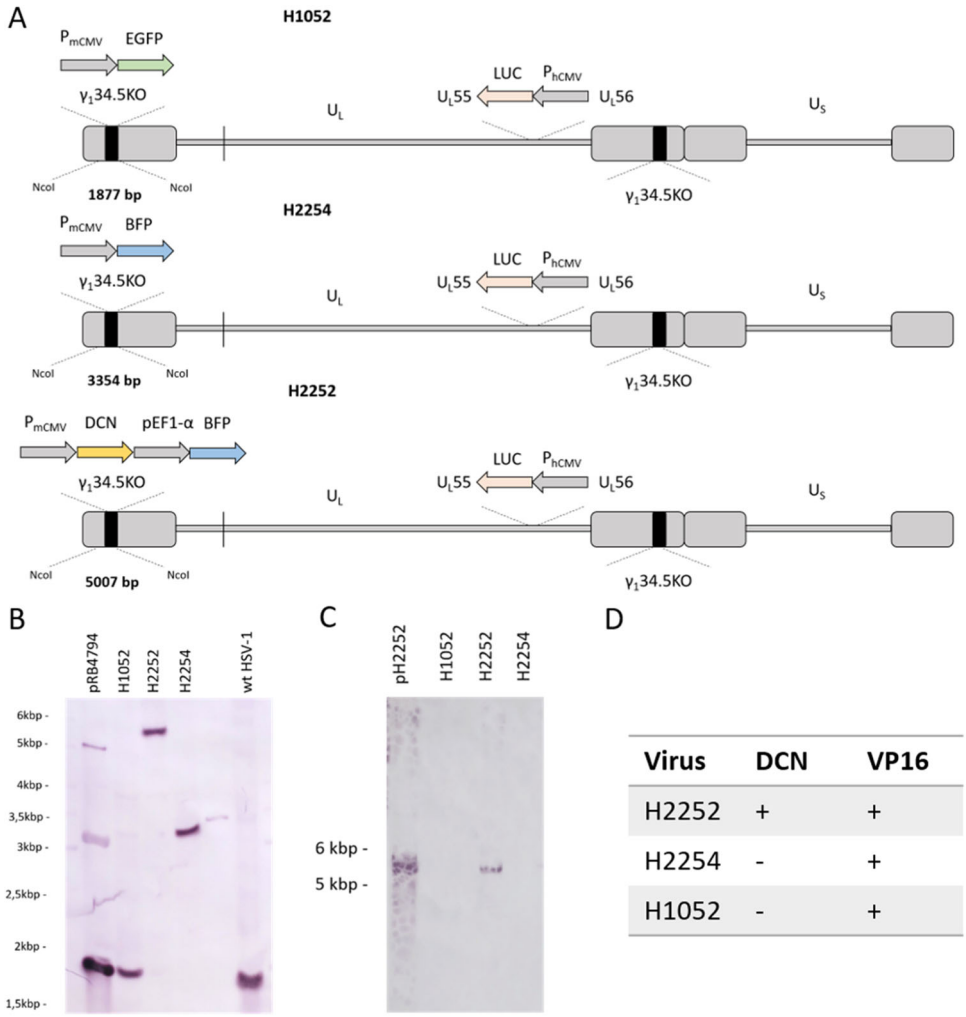

FIGURE 1 | (A) Simplified diagram of the transgenes and knockouts (KO) in the three HSV vectors. LUC stands for luciferase. The predicted sizes of the hybridized NcoI fragments are indicated underneath the TR_L region of the genome. (B) Southern blot of cytoplasmic DNA extracted from infected cells. The DNA was digested with NcoI, electrophoretically separated and transferred to a nylon membrane and hybridized with a digoxigenin (DIG)-labeled 1.8 kb NcoI fragment of HSV-1 DNA from plasmid pRB4794. The predicted fragment sizes are 1.8 kbp for H1052, 5 kbp for H2252 and 3.3 kbp for H2254 as well as 1.8 kbp for wild type HSV-1 (previously published as V3 [36]). (C) DCN Southern blot of cytoplasmic viral DNA extracted from the infected cells. As previously, the DNA was digested by NcoI, electrophoretically separated and transferred to a nylon membrane and hybridized with a DIG-labeled 533 bp DCN fragment. The positive control for DCN is pH2252 which was used for construction of H2252. (D) The presence of the DCN gene verified by PCR from the viral DNA extracted from the supernatant-derived virus.

supernatant was collected and centrifuged in a Beckman Avanti centrifuge with a JA-14 rotor at 16 300 rcf +4°C for 1.5 h, after which the supernatant was removed and the pellet resuspended in MNT buffer (20 mM MES (Sigma-Aldrich, St. Louis, MO, USA), 100 mM NaCl, and 30 mM Tris, pH 7.4) overnight [39]. The titers were determined with plaque titration in Vero cells as described later.

2.3 | Plaque Titration

To determine the viral titers the sample was diluted in a tenfold series on confluent Vero cells in 96-well plates. At 1 h post infection, the medium was overlaid with DMEM supplemented with 7% FBS, gentamycin and 40 mg/mL immunoglobulin G (HyQvia, Takeda, Tokyo, Japan). The supernatant was removed and the cells were fixed with methanol and stained with crystal violet 72 h post infection. The primary plaques were then counted.

2.4 | Viral Genomic PCR

Viral MNT stocks were heated to 98°C for 10 min. PCR was performed using the SybrGreen enzyme system (Thermo Fisher Scientific) and Rotor-Gene instrument (Qiagen, Hilden, Germany) as previously described [40]. DCN and VP16 gene copies were determined. Primer information has been published previously [29, 41].

2.5 | Southern Blot

Cytoplasmic DNA was extracted from the infected Vero cells that had reached full cytopathic effect. The extraction was performed by adding lysis buffer (150 mM NaCl, 10 mM Tris pH 7.5, 1.5 mM MgCl, 0.1% NP-40) to pelleted cells. The solution was gently centrifuged, the cytoplasm (supernatant) collected, and the pellet (cellular nuclei) discarded. The cytoplasm

was treated in a solution of 0.4% (V/V) beta-mercaptoethanol and 1% (V/V) 0.5 M EDTA pH 8.0. The cytoplasm was phenol:chlorophorm:isoamylalcohol extracted three times and then the DNA was ethanol precipitated and resuspended in double distilled sterile water.

The DNA was digested with Fast Digest NcoI (Thermo Fisher Scientific) using the manufacturer's protocol and separated on a 0.8% agarose gel for 24 h (30 V 0.01 A). A 1kbp DNA plus ladder (Thermo Fisher Scientific) was used. The DNA was transferred onto a Zeta probe membrane (Bio-Rad, California, US) overnight using alkaline transfer buffer (0.4 M NaOH, 1.5 M NaCl) and then neutralized in 0.5 M Tris pH 7.5/1.5 M NaCl. The membrane was then hybridized with a digoxigenin-labeled 1.8 kb NcoI-NcoI subfragment of the BamHI S fragment of HSV-1 DNA (pRB4794) [42, 43] or a 533 bp DCN fragment [44], which were labeled using the DIG DNA labeling and detection kit (Sigma-Aldrich, Missouri, US), and detected using NBT/BCIP stain (Sigma-Aldrich) according to the manufacturer's instructions.

2.6 | Western Blot

Subconfluent T-25 flasks of A549 cells were infected with 0.1 MOI of each virus and samples were collected 48 h post infection by scraping the cells into the medium, and pelleted at 2500 rcf for 5 min at +4°C. The supernatant was aspirated, and the pellet dissolved in lysis buffer (50 mM Tris-HCL, pH 7.4, 150 mM NaCl, 5 mM EDTA, 1% NP-40, 0.1% SDS, proteinase inhibitor added before use).

The quantifying of sample protein concentration was determined using Pierce™ BCA Protein Assay Kit (Thermo Fisher Scientific). The samples were mixed with 2× Laemmli Sample Buffer (Bio-Rad) containing dithiothreitol as a reducing agent and heated to 98°C for 5 min to denature. A total of 5 μg of protein was loaded per sample for the SDS-PAGE.

Electrophoretic separation was performed on a 4–15% Mini-PROTEAN TGX precast protein gel (Bio-Rad) (to optimize the resolution of target proteins falling within the range of 30–65 kDa) at 90 V. Following electrophoresis, protein transfer to 0.45 μm PVDF membrane (Thermo Fisher Scientific) was achieved by a wet transfer setup on a block of ice. The membranes were blocked with EveryBlot Blocking Buffer (Bio-Rad) to reduce non-specific binding and then incubated with specific primary antibodies against DCN (Abcam, Cambridge, UK) or glycoprotein D (gD) (Santa Cruz Biotechnology, Texas, US), and GAPDH (Invitrogen, Massachussets, US) diluted 1:1000 in blocking buffer. To detect these primary antibodies, HRP-conjugated secondary antibodies (Invitrogen) were used and incubated at room temperature for 1 h. The visualization of protein bands was done using SuperSignal West Femto Maximum Sensitivity Substrate (Thermo Fisher Scientific) and chemiluminescent signals were imaged using an iBright CL1500 Imaging System (Thermo Fisher Scientific). Protein loading was normalized to GAPDH. Densitometric analysis was performed using the iBright CL1500 and ImageJ software, providing quantitative data on protein expression.

2.7 | Immunofluorescence

A549 cells seeded on 96-well plates were infected with 1 MOI of H2252 or H2254 and after 24 h fixed with 4% paraformaldehyde added to the medium 1:1 for 20 min. The supernatant was then aspirated, and the fixed cells washed with PBS. The fixed cells were permeabilized with 50 μL of 0.1% Triton X-100 for 5 min before they were incubated with a primary DCN antibody (Abcam; 1:2000 dilution) in 3% BSA for 1 h at room temperature. The cells were then washed three times with 0.5% BSA for 5 min. Following this, the cells were incubated with a secondary antibody (Alexa fluor 488 goat anti-rabbit/guinea pig IgG; 1:1000 dilution) and DAPI (1:2500 dilution) in 3% BSA for 1 h in room temperature. The cells were washed as previously and incubated for 30 min before imaging with the EVOS FL auto imaging system (Thermo Fisher Scientific). Due to the green fluorescence of the secondary antibody, the GFP-expressing virus H1052 was not included in this study.

2.8 | Cell-Bound Versus Released Virus

A549 cells were seeded onto 96-well plates and when 90% confluent the medium was changed to DMEM supplemented with 2% FBS and gentamycin. Virus stocks were diluted to 5 MOI and added onto the cells. After 1 h, the cells were washed with PBS and medium replaced to DMEM supplemented with 7% FBS, gentamycin and GlutaMAX. For each repeat experiment, the titer of the viral stock was redetermined. The supernatants were collected, and the cells covered in 100 μL 9% milk at 24 h post infection. The samples were stored at −80°C. The cells were freeze thawed three times. The titers of the cellular and supernatant samples were then determined using plaque titration. The experiment was repeated three additional times with 5 parallel wells per treatment.

2.9 | Viral Growth Curve

A549 cells were seeded onto 96-well plates, and when 90% confluent the medium was changed to DMEM supplemented with 2% FBS and gentamycin. Virus stocks were diluted to 5 MOI and added to the cells. After 1 h, the cells were washed with PBS and medium replaced to DMEM supplemented with 7% FBS, gentamycin and GlutaMAX. For each repeat experiment, the titer of the viral stock was redetermined. 20 μL of supernatant was collected from each well at 6, 24, 48, and 72 h post infection and stored at −80°C. After collecting the supernatant, medium was added to replace the removed medium. The titers were then determined using plaque titration. The experiment was repeated three additional times with five parallel wells per treatment.

2.10 | Cytotoxicity Assay

The oncolytic potential of the viruses (cytotoxicity) was determined using an MTT viability assay in a 96-well plate. A549 cells were seeded onto 96-well plates and when 90% confluent the medium was changed to DMEM supplemented with 2% FBS

and gentamycin. Virus stocks were diluted to either 5, 1, or 0.3 MOI and added onto the cells. For each repeat experiment, the titer of the viral stock was redetermined. After 1 h, the cells were washed with PBS and medium replaced to DMEM supplemented with 7% FBS, gentamycin and GlutaMAX. After infections, 15 μL MTT (Promega CellTiter Nonradioactive cell proliferation assay, Thermo Fisher Scientific) was added to the wells 24, 48 and 72 h post infection according to the manufacturer's protocol. After 3 h, the reactions were visually determined to be saturated, and 100 μL of stopping solution were added per well. The dye was left to dissolve protected from light overnight, after which the plate was shaken for 1 min in 300 orbits/min and the absorbance was determined using a Victor Nivo multimode plate reader (PerkinElmer. Massachusetts, US). The wavelength of 570/10 nm was quantified and the wavelength 665/8 nm was used as a reference. The recordings from the reference wavelength were then subtracted from the recordings from the optimal wavelength. The experiment was repeated three additional times with 5 parallel wells per treatment.

2.11 | Gene Expression RT-qPCR

A549 cells were seeded onto 96-well plates and when 90% confluent the medium was changed to DMEM supplemented with 2% FBS and gentamycin. Virus stocks were diluted to 5 MOI and added onto the cells. After 1 h, the cells were washed with PBS and medium replaced to DMEM supplemented with 7% FBS, gentamycin and GlutaMAX. 24 h post infection the supernatant was removed, cells were overlaid with 80 μL Tri Reagent (Thermo Fischer Scientific), and the RNA was extracted according to the manufacturer's protocol. Complementary DNA was synthesized from the DNA with RevertAid H Reverse Transcriptase (Thermo Fisher Scientific) and random hexamer primers (Thermo Fisher Scientific) as described previously [40]. RT-qPCR was performed as described earlier. Standard and calibrator information has been published previously [41, 45–48]. In addition to DCN gene expresssion, the expression of the viral VP16 and gD single copy genes and the GAPDH housekeeping gene were determined.

2.12 | Statistical Analysis

The statistical significance (Mann–Whitney *U*) was calculated using SPSS statistics (IBM).

3 | Results

3.1 | Recombinant HSV Vectors

We constructed two novel recombinant vectors using a transfection-infection method and marker selection using a GFP backbone virus H1052 [38]: H2252, a DCN and a BFP expressing virus; and H2254, a BFP expressing virus. The recombination was confirmed upon observation of BFP positive/GFP negative plaques. Viral stocks were prepared when no GFP was present for two subsequent plaque purification rounds. The location of the insert in the viral genome was verified using Southern blot, where the probe was a digoxigenin-labeled 1.8 kbp NcoI-NcoI subfragment of BamHI S fragment of HSV-1 DNA (pRB4794) [42, 43]. The probe hybridized to flanks of the deletion in the $\gamma_1$34.5 gene (Figure 1B). The predicted sizes are shown in Figure 1A, and are 1877 for H1052, 5007 bp for H2252 and 3354 bp for H2254. The fragments in all three viruses corresponded with their predicted sizes (Figure 1A,B). The presence of the DCN insert in H2252 was verified using Southern blot with a 533 bp DCN probe (Figure 1C) and PCR for detecting the DCN gene in the viral genome (Figure 1D). Only H2252 had the DCN gene present (Figure 1D), while detection of VP16 gene DNA validated the viral DNA in the PCR samples.

3.2 | DCN Expression of the Recombinant Virus

The DCN expression by A549 cells infected with H2252 was assessed. RT-qPCR revealed that A549 cells infected with H2252 express significantly more DCN mRNA than uninfected A549 cells 24 h post infection ($p < 0.05$), and infection with H1052 or H2254 did not alter DCN expression (Figure 2A). We could also detect the intracellular DCN core protein in H2252-infected cells using immunofluorescence 24 h post infection (Figure 2C). Western blot analysis revealed that A549 cells infected with H2252 produce the DCN core protein of about 50 kDa (Figure 2D). Uninfected A549 cells produce neither DCN core protein nor express DCN mRNA (Figure 2A,D). Both western blot analysis (standardized to total protein quantity) and RT-qPCR reveal that A549 cells infected with H1052 express more gD and GAPDH than those infected with H2252 or H2254 (Figure 2B,E).

The course of infection with the HSV recombinants in A549 cells did not differ significantly. The BFP intensity differed between H2254 and H2252 (Figure 3A). The released virus in the supernatant of all vectors peaked at 24 h post infection (Figure 3B). The ratio of released virions to that of cell bound virus varied between 30% and 38% depending on the recombinant (Figure 3C).

3.3 | Oncolytic Activity of the Recombinant Vectors

Oncolytic efficacy was measured as cytotoxicity (decrease in cell viability) using the MTT viability assay. All three viral doses of H2252 at 48 h post infection display more oncolytic efficacy than H1052 or H2254 ($p < 0.05$) (Figure 4A,B). At 24 h post infection H2252 is more efficacious than H1052 at 1 MOI, and at 72 h post infection H2252 is more efficacious than H1052 at 1 MOI and both H2252 and H1052 are more efficacious than H2254 at 5 MOI ($p < 0.05$) (Figure 4A,B). The cytopathic effect of H2252 infection during the assay is visualized in Figure 4D compared to uninfected control in Figure 4C. Infections with H2254 and H1052 were visually indistinguishable from H2252.

4 | Discussion

As lung adenocarcinoma is a leading cause of cancer-related mortality despite advances in modern treatments, novel

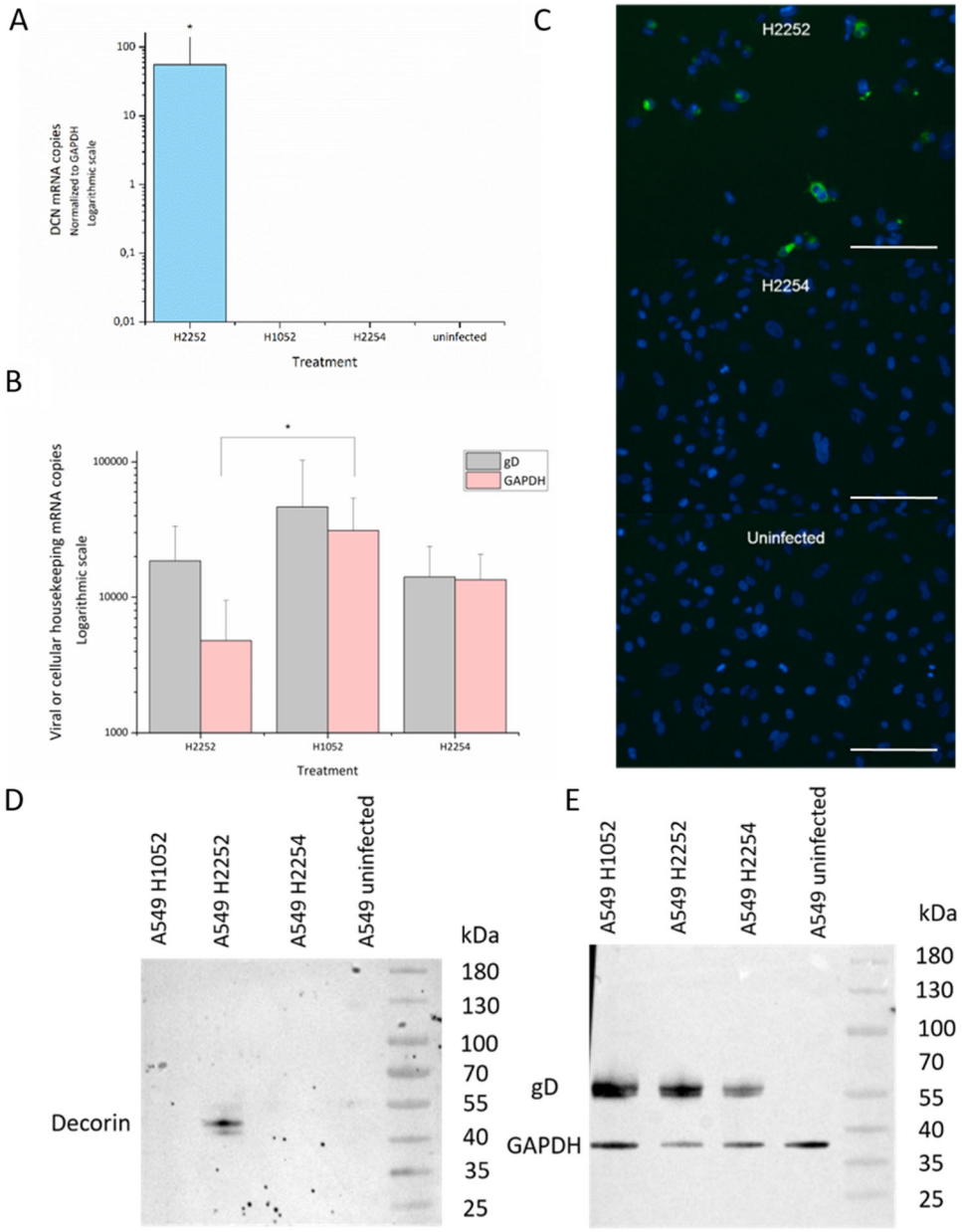

FIGURE 2 | (A, B) RT-qPCR of samples collected from A549 cells 24 h post infection. $N = 5$. (A) DCN mRNA expression normalized to GAPDH. (B) GAPDH and viral glycoprotein D (gD) expression. The capped bars represent standard deviation, the asterisks represent statistical significance ($p < 0.05$). (C) Immunofluorescence of paraformaldehyde fixed infected cells. Images taken with EVOS FL auto imaging system. Blue fluorescence (DAPI) represents the cellular nuclei and green fluorescence represents the DCN core protein. The scale bar represents 200 μm. (D, E) Western blot of samples collected from A549 48 h post infection. Lysed samples of infected cells were electrophoretically separated and detected with either DCN, gD or GAPDH antibodies. The same blot is illustrated in both images, the left image showing DCN and the right gD and GAPDH.

therapies need to be discovered. DCN, an extracellular proteoglycan that is important in regulating many processes in the connective tissue, is often not expressed in lung adenocarcinoma [49]. DCN has previously been found to suppress tumor growth and pathways. Thus, we constructed an oncolytic HSV-1 vector that expresses DCN to assess its feasibility as a treatment against lung adenocarcinoma.

For the construction of the oncolytic virus DCN vector H2252 as well as a control vector H2254, we designed two plasmids with flanks homologous with the neurovirulence gene of HSV, present in the parental strain H1052, surrounding the expression cassette. The new vectors were created using a transfection-infection recombination and selection based on the marker gene expression, where successful recombination was found by replacement of green fluorescence with blue fluorescence. The difference in blue fluorescence intensity between the cells infected with H2252 and H2254 (Figure 3A) is most likely due to the BFP gene being regulated by different promoters of varying transcription efficiency (Figure 1A).

The presence of DCN in the genome of H2252 was verified with genomic PCR and Southern blot (Figure 1B–D). The absence of DCN copies in the samples from H1052 and H2254 show that

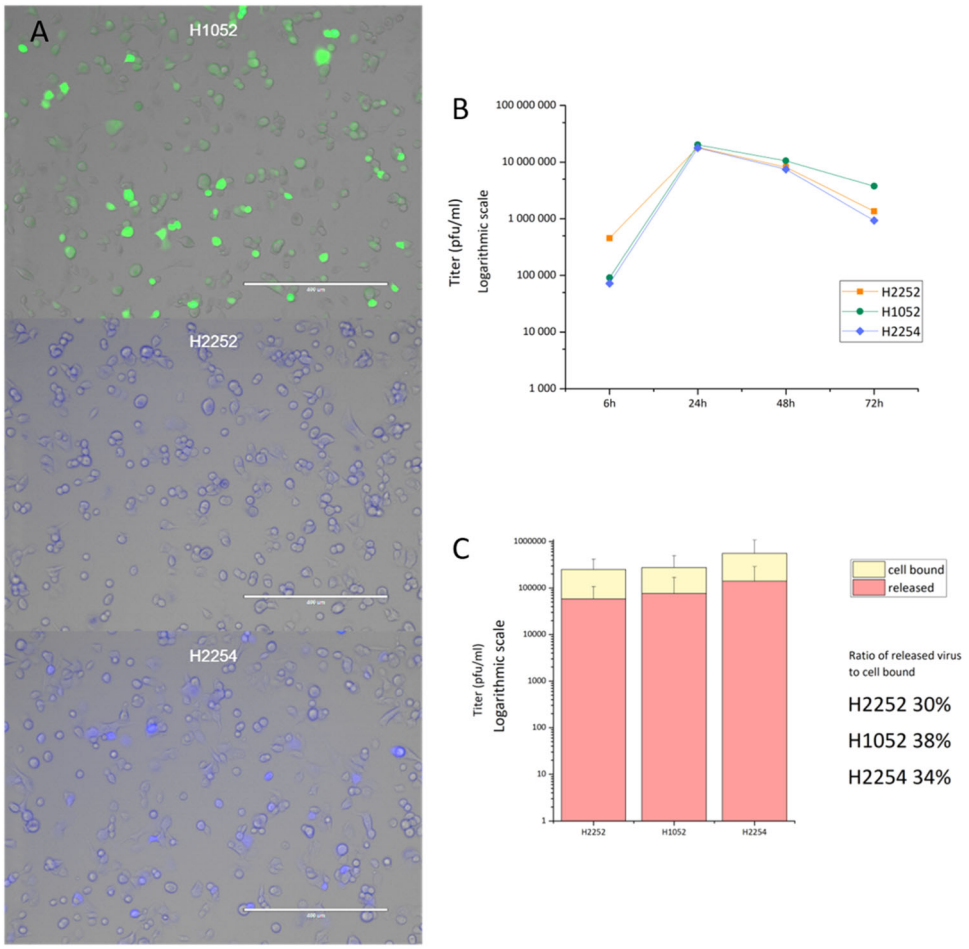

FIGURE 3 | (A) Fluorescence images of infected A549 cells. GFP, BFP and transmitted light channels are all overlaid in each image. H1052 infected cells express GFP while H2254 and H2252 infected cells express BFP. The scale bar represents 400 μm. (B, C) Virus growth in A549 cells. $N = 20$. (B) Growth curve of released virus determined during a 72 h period. (C) Released and cell bound viral titers 24 h post infection. The percentages represent the ratio of released virus to cell bound virus. The capped bars represent standard deviation.

the host DCN gene is not present in the viral stock used as the source material (Figure 1D). Southern blot confirmed the location of the insert in the genome, as the hybridized 1.8 kbp NcoI fragment of the HSV-1 BamHI fragment S labeled the correct predicted location, and the DCN fragment hybridized with the same predicted fragment (Figure 1B,C). Western blot analysis shows that mRNA detected with RT-qPCR (Figure 2A) is translated correctly (Figure 2D). These results also show that the infection with the HSV viruses H1052 and H2254 does not induce DCN expression in A549 cells, and that A549 cells have no native DCN expression (Figure 2A,D). These results correlate with other observations that lung adenocarcinoma often has underexpressed DCN [49]. The western blot analysis shows that A549 cells infected with H2252 express DCN core protein. Immunofluorescence detected intracellular DCN core protein in H2252 infected A549 cells (Figure 2C).

Interestingly, RT-qPCR paradoxically shows higher copy numbers of both gD and GAPDH in A549 cells infected with H1052 than with H2252 or H2554 (Figure 2B). It could be argued that more surviving cells would express more gD copies, however Western blot analysis from different samples shows the same phenomenon when normalized to protein quantity, suggesting that more cells are viable even though more viral protein is expressed (Figure 2E). This evidence suggests that H1052 is less oncolytic than its corresponding BFP expressing counterpart H2254 as well as the DCN expressing H2252. This difference could be due to GFP, or the selective passaging of H2252 and H2254 in BHK21-13s cells causing subtle phenotype changes in the virus. However, the cytoplasmic viral DNA fragment sizes do not indicate any additional differences between the parental virus H1052 and H2252 or H2254 than the one detected by Southern blot.

The growth curve and shed vs cell bound titers in A549 cells show that the addition of a large expression cassette with DCN does not alter the course of infection in a detectable manner (Figure 3). However, the MTT viability assay shows that DCN significantly increases the oncolytic activity of the vector compared to the control and parental viruses, especially at 48 h post infection with all MOIs tested (Figure 4A,B). This oncolytic activity plateaus at 60%, where the limit of this quantitative assay for oncolytic efficacy is reached. While visual analysis of the cells shows a full cytopathic effect (Figure 4C,D), the assay gives a higher viability readout as the cells have high metabolic capacity when they are producing progeny virions, but the cells

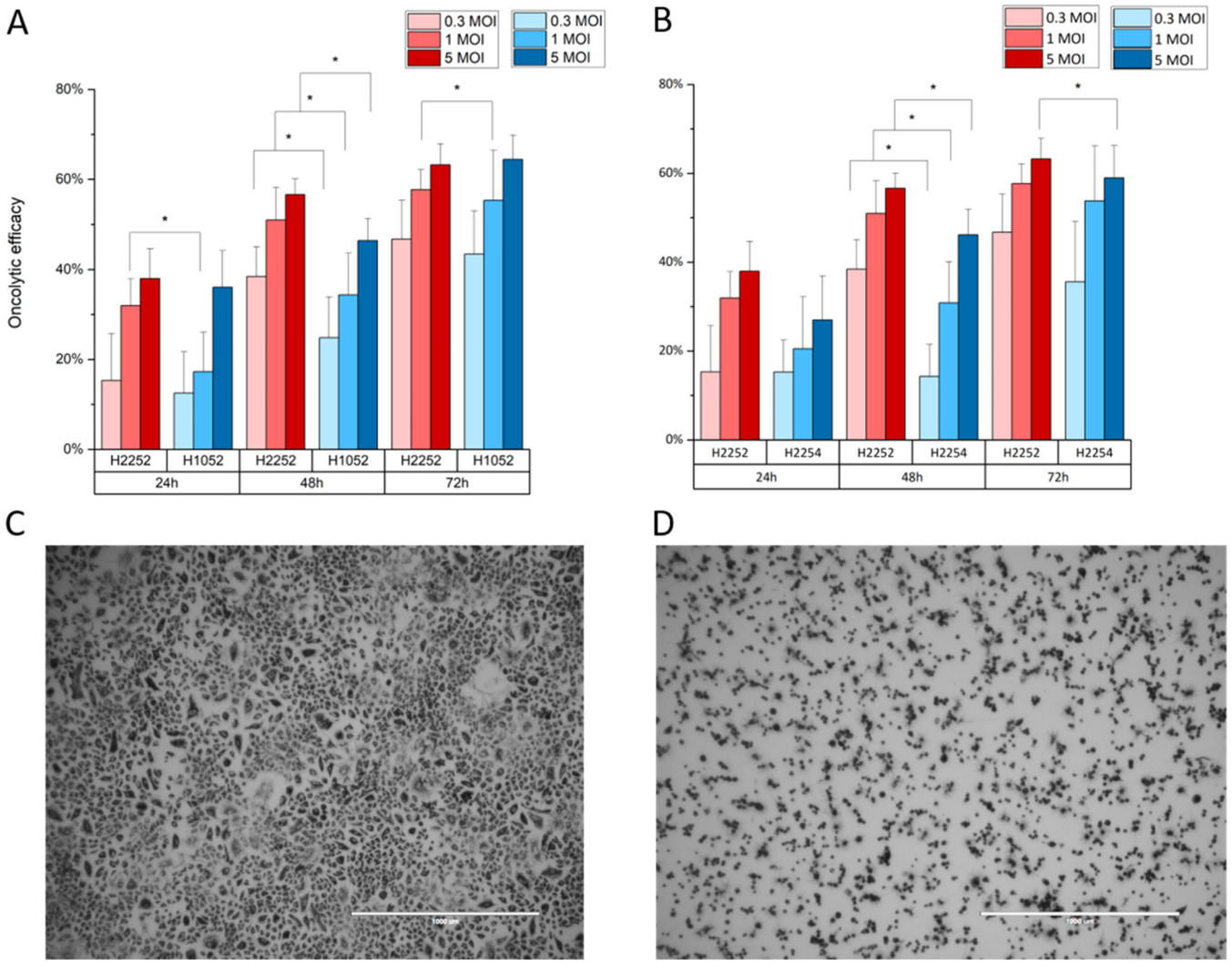

FIGURE 4 | Comparison of oncolytic efficacy, or cytotoxicity, of the recombinant viruses in A549 cells, as measured using MTT viability assay. $N = 20$. (A) Comparison of parental virus H1052 and DCN expressing H2252. (B) Comparison of control virus H2254 and DCN expressing H2252. The capped bars represent the standard deviation and the asterisk represents statistical significance (*$p < 0.05$). (C, D). Images of the cells incubated with MTT before solubilization. (C) Uninfected A549 cells. (D) A549 cells 24 h post infection infected with 5 MOI of H2252. Infection with control viruses were visually similar to H2252. The scale bar represents 1000 μm.

cannot in fact proliferate. This is a limitation of all in vitro viability assays when applied to infected cells [50].

Our novel recombinant virus is the first HSV expressing DCN to our knowledge, and our replication competent HSV has the advantage of only requiring low MOI dosages for high in vitro efficacy. Furthermore, HSV vectors have clinically been proven suitable for repeat dosing and low toxicity [28]. Our results are also in line with previous studies using DCN gene therapy against tumors, where DCN improved the oncolytic efficacy of other viral vectors [24–26]. Although the evidence of the new DCN oncolytic vector's superiority is limited to in vitro results, we propose that these results support the further development of a DCN expressing oncolytic HSV-1 vector for studies in in vivo models for the treatment of lung adenocarcinoma. For delivery of our novel vector to lungs, we have in conjunction with a previous study expressed transgenes in the lungs of mice administered with recombinant HSV intranasally [35]. We deem that this would be a suitable administration method for future in vivo studies.

Author Contributions

Conceptualization: Hannu Järveläinen, Veijo Hukkanen; methodology, Fanny Frejborg, Jussi Palomäki, Kiira Kalke, Julius Orpana, Oliver Koivisto, Henrik Paavilainen, Veijo Hukkanen. Formal analysis: Fanny Frejborg, Jussi Palomäki, Oliver Koivisto, Veijo Hukkanen. Investigation: Fanny Frejborg, Jussi Palomäki, Kiira Kalke, Julius Orpana, Oliver Koivisto, Veijo Hukkanen. Resources: Fanny Frejborg, Kiira Kalke, Veijo Hukkanen. Data curation: Fanny Frejborg. Writing—original draft preparation: Fanny Frejborg. Writing—review and editing: Fanny Frejborg, Jussi Palomäki, Kiira Kalke, Julius Orpana, Oliver Koivisto, Henrik Paavilainen, Jessica M. Rosenholm, Hongbo Zhang, Hannu Järveläinen, Veijo Hukkanen. Visualization: Fanny Frejborg, Oliver Koivisto. Supervision: Kiira Kalke, Henrik Paavilainen, Jessica M. Rosenholm, Hongbo Zhang, Hannu Järveläinen, Veijo Hukkanen. Project administration: Henrik Paavilainen, Jessica M. Rosenholm, Hongbo Zhang, Hannu Järveläinen, Veijo Hukkanen. Funding acquisition: Henrik Paavilainen, Jessica M. Rosenholm, Hongbo Zhang, Hannu Järveläinen, Veijo Hukkanen. All authors have read and accepted the published version of the manuscript.

Acknowledgments

We thank Soili Jussila at CellCore for the upkeep of the cell stocks. We acknowledge Dr. Wenhui Zhou, Dr. Pekka Kolehmainen, Anja Hjelt, Dr. Roope Huttunen and Salla Alaollitervo (Åbo Akademi University and University of Turku, Turku, Finland) for their supportive aid in this project. The plasmid pRB4794 was a generous gift from Prof. Bernard Roizman, University of Chicago, Chicago, USA. F.F. would like to thank Åbo Akademi University Graduate School for personal funding in the form of PhD salary. The authors would further like to thank the Jane and Aatos Erkko foundation (#170046), Satasairaala Central Hospital, The Wellbeing Services County of Satakunta, Cancer Foundation of Southwestern Finland, State of Finland Research Fund (VTR), Research Council of Finland (project numbers #337531, #347897, #353146), Sigrid Jusélius foundation, The Paulo Foundation and Turku University foundation for funding this project. J.P. would like to thank The Finnish Cultural Foundation, South Ostrobothnia Regional Fund (grant number 10231545), Cancer Association of South-Western Finland (grant date 20211210) and Kauhajoki Cultural Foundation (grant date 20230421) for personal funding. K.K. and V.H. have also been supported by the research project 26004913 from Orion Pharma, Finland. This research is also aligned with the strategic research profiling area "Solutions for Health" at Åbo Akademi University (funded by the Research Council of Finland, #336355).

Ethics Statement

The virus construction and use were according to the notifications 018/M/2018 and 008/M/2020 of the National Board of Gene Technology of Finland.

Conflicts of Interest

Orion Corporation has supported the construction of the marker virus H2254. H.P. was employed by Orion Corporation during this project. The other authors declare no conflicts of interest.

Data Availability Statement

The data that support the findings of this study are available from the corresponding author upon reasonable request.

References

1. F. Bray, M. Laversanne, H. Sung, et al., "Global Cancer Statistics 2022: GLOBOCAN Estimates of Incidence and Mortality Worldwide for 36 Cancers in 185 Countries," *CA: A Cancer Journal for Clinicians* 74, no. 3 (2024): 229–263, https://doi.org/10.3322/caac.21834.

2. J. H. Bi, J. Y. Tuo, Y. X. Xiao, et al., "Observed and Relative Survival Trends of Lung Cancer: A Systematic Review of Population-Based Cancer Registration Data," *Thoracic Cancer* 15, no. 2 (2024): 142–151, https://doi.org/10.1111/1759-7714.15170.

3. C. I. Lorda-Diez, J. A. García-Porrero, J. M. Hurlé, and J. A. Montero, "Decorin Gene Expression in the Differentiation of the Skeletal Connective Tissues of the Developing Limb," *Gene Expression Patterns* 15, no. 1 (2014): 52–60, https://doi.org/10.1016/j.gep.2014.04.003.

4. L. Häkkinen, J. Westermarck, V. M. Kähäri, and H. Larjava, "Human Granulation-Tissue Fibroblasts Show Enhanced Proteoglycan Gene Expression and Altered Response to TGF-β1," *Journal of Dental Research* 75, no. 10 (1996): 1767–1778, https://doi.org/10.1177/00220345960750101001.

5. C. Velez-DelValle, M. Marsch-Moreno, F. Castro-Muñozledo, and W. Kuri-Harcuch, "Decorin Gene Expression and Its Regulation in Human Keratinocytes," *Biochemical and Biophysical Research Communications* 411, no. 1 (2011): 168–174, https://doi.org/10.1016/j.bbrc.2011.06.122.

6. A. E. Redington, W. R. Roche, S. T. Holgate, and P. H. Howarth, "Co-Localization of Immunoreactive Transforming Growth Factor-Beta 1 and Decorin in Bronchial Biopsies From Asthmatic and Normal Subjects," *Journal of Pathology* 186, no. 4 (1998): 410–415, https://doi.org/10.1002/(SICI)1096-9896(199812)186:4<410::AID-PATH198>3.0.CO;2-9.

7. L. Nelimarkka, H. Salminen, T. Kuopio, et al., "Decorin Is Produced by Capillary Endothelial Cells in Inflammation-Associated Angiogenesis," *American Journal of Pathology* 158, no. 2 (2001): 345–353, https://doi.org/10.1016/S0002-9440(10)63975-2.

8. K. Baghy, R. V. Iozzo, and I. Kovalszky, "Decorin-TGFβ Axis in Hepatic Fibrosis and Cirrhosis," *Journal of Histochemistry & Cytochemistry* 60, no. 4 (2012): 262–268, https://doi.org/10.1369/0022155412438104.

9. S. F. Penc, B. Pomahac, T. Winkler, et al., "Dermatan Sulfate Released after Injury Is a Potent Promoter of Fibroblast Growth Factor-2 Function," *Journal of Biological Chemistry* 273, no. 43 (1998): 28116–28121, https://doi.org/10.1074/jbc.273.43.28116.

10. N. Nili, A. N. Cheema, F. J. Giordano, et al., "Decorin Inhibition of PDGF-Stimulated Vascular Smooth Muscle Cell Function," *American Journal of Pathology* 163, no. 3 (2003): 869–878, https://doi.org/10.1016/S0002-9440(10)63447-5.

11. M. Santra, C. C. Reed, and R. V. Iozzo, "Decorin Binds to a Narrow Region of the Epidermal Growth Factor (EGF) Receptor, Partially Overlapping but Distinct From the EGF-Binding Epitope," *Journal of Biological Chemistry* 277, no. 38 (2002): 35671–35681, https://doi.org/10.1074/jbc.M205317200.

12. G. Nareyeck, D. G. Seidler, D. Troyer, J. Rauterberg, H. Kresse, and E. Schönherr, "Differential Interactions of Decorin and Decorin Mutants With Type I and Type VI Collagens," *European Journal of Biochemistry* 271, no. 16 (2004): 3389–3398, https://doi.org/10.1111/j.1432-1033.2004.04273.x.

13. B. Han, Q. Li, C. Wang, et al., "Decorin Regulates the Aggrecan Network Integrity and Biomechanical Functions of Cartilage Extracellular Matrix," *ACS Nano* 13, no. 10 (2019): 11320–11333, https://doi.org/10.1021/acsnano.9b04477.

14. D. R. Chery, B. Han, Y. Zhou, et al., "Decorin Regulates Cartilage Pericellular Matrix Micromechanobiology," *Matrix Biology* 96 (2021): 1–17, https://doi.org/10.1016/j.matbio.2020.11.002.

15. Q. Li, B. Han, C. Wang, et al., "Mediation of Cartilage Matrix Degeneration and Fibrillation by Decorin in Post-Traumatic Osteoarthritis," *Arthritis & Rheumatology* 72, no. 8 (2020): 1266–1277, https://doi.org/10.1002/art.41254.

16. B. Han, Q. Li, C. Wang, et al., "Differentiated Activities of Decorin and Biglycan in the Progression of Post-Traumatic Osteoarthritis," *Osteoarthritis and Cartilage* 29, no. 8 (2021): 1181–1192, https://doi.org/10.1016/j.joca.2021.03.019.

17. S. P. Reese, C. J. Underwood, and J. A. Weiss, "Effects of Decorin Proteoglycan on Fibrillogenesis, Ultrastructure, and Mechanics of Type I Collagen Gels," *Matrix Biology* 32, no. 7–8 (2013): 414–423, https://doi.org/10.1016/j.matbio.2013.04.004.

18. S. N. Giri, D. M. Hyde, R. K. Braun, W. Gaarde, J. R. Harper, and M. D. Pierschbacher, "Antifibrotic Effect of Decorin in a Bleomycin Hamster Model of Lung Fibrosis," *Biochemical Pharmacology* 54, no. 11 (1997): 1205–1216, https://doi.org/10.1016/s0006-2952(97)00343-2.

19. H. Järveläinen, P. Puolakkainen, S. Pakkanen, et al., "A Role for Decorin in Cutaneous Wound Healing and Angiogenesis," *Wound Repair and Regeneration* 14, no. 4 (2006): 443–452, https://doi.org/10.1111/j.1743-6109.2006.00150.x.

20. K. Baghy, K. Dezső, V. László, et al., "Ablation of the Decorin Gene Enhances Experimental Hepatic Fibrosis and Impairs Hepatic Healing in Mice," *Laboratory Investigation* 91, no. 3 (2011): 439–451, https://doi.org/10.1038/labinvest.2010.172.

21. K. Sylakowski, M. P. Hwang, A. Justin, D. Whaley, Y. Wang, and A. Wells, "The Matricellular Protein Decorin Delivered Intradermally

With Coacervate Improves Wound Resolution in the CXCR3-deficient Mouse Model of Hypertrophic Scarring," *Wound Repair and Regeneration* 30, no. 4 (2022): 436–447, https://doi.org/10.1111/wrr.13017.

22. D. G. Seidler, S. Goldoni, C. Agnew, et al., "Decorin Protein Core Inhibits in Vivo Cancer Growth and Metabolism by Hindering Epidermal Growth Factor Receptor Function and Triggering Apoptosis via caspase-3 Activation," *Journal of Biological Chemistry* 281, no. 36 (2006): 26408–26418, https://doi.org/10.1074/jbc.M602853200.

23. D. S. Grant, C. Yenisey, R. W. Rose, M. Tootell, M. Santra, and R. V. Iozzo, "Decorin Suppresses Tumor Cell-Mediated Angiogenesis," *Oncogene* 21, no. 31 (2002): 4765–4777, https://doi.org/10.1038/sj.onc.1205595.

24. A. R. Yoon, J. Hong, and C. O. Yun, "Adenovirus-Mediated Decorin Expression Induces Cancer Cell Death through Activation of p53 and Mitochondrial Apoptosis," *Oncotarget* 8, no. 44 (2017): 76666–76685, https://doi.org/10.18632/oncotarget.20800.

25. C. Zhang, L. Fang, X. Wang, et al., "Oncolytic Adenovirus-Mediated Expression of Decorin Facilitates CAIX-Targeting CAR-T Therapy Against Renal Cell Carcinoma," *Molecular Therapy—Oncolytics* 24 (2022): 14–25, https://doi.org/10.1016/j.omto.2021.11.018.

26. C. C. Reed, J. Gauldie, and R. V. Iozzo, "Suppression of Tumorigenicity by Adenovirus-Mediated Gene Transfer of Decorin," *Oncogene* 21, no. 23 (2002): 3688–3695, https://doi.org/10.1038/sj.onc.1205470.

27. T. Zhang, T. H. T. Jou, J. Hsin, et al., "Talimogene Laherparepvec (T-VEC): A Review of the Recent Advances in Cancer Therapy," *Journal of Clinical Medicine* 12, no. 3 (2023): 1098, https://doi.org/10.3390/jcm12031098.

28. R. H. I. Andtbacka, H. L. Kaufman, F. Collichio, et al., "Talimogene Laherparepvec Improves Durable Response Rate in Patients With Advanced Melanoma," *Journal of Clinical Oncology* 33, no. 25 (2015): 2780–2788, https://doi.org/10.1200/JCO.2014.58.3377.

29. E. K. Broberg, J. Peltoniemi, M. Nygårdas, T. Vahlberg, M. Röyttä, and V. Hukkanen, "Spread and Replication of and Immune Response to γ134.5-Negative Herpes Simplex Virus Type 1 Vectors in BALB/c Mice," *Journal of Virology* 78, no. 23 (2004): 13139–13152, https://doi.org/10.1128/JVI.78.23.13139-13152.2004.

30. B. He, M. Gross, and B. Roizman, "The Gamma(1)34.5 Protein of Herpes Simplex Virus 1 Complexes With Protein Phosphatase 1Alpha to Dephosphorylate the Alpha Subunit of The Eukaryotic Translation Initiation Factor 2 and Preclude the Shutoff Of Protein Synthesis by Double-Stranded RNA-Activated Protein Kinase," *Proceedings of the National Academy of Sciences of the United States of America* 943 (1997): 843–848, https://doi.org/10.1073/pnas.94.3.843.

31. A. Orvedahl, D. Alexander, Z. Tallóczy, et al., "HSV-1 ICP34.5 Confers Neurovirulence by Targeting the Beclin 1 Autophagy Protein," *Cell Host & Microbe* 1, no. 1 (2007): 23–35, https://doi.org/10.1016/j.chom.2006.12.001.

32. D. Verpooten, Y. Ma, S. Hou, Z. Yan, and B. He, "Control of TANK-Binding Kinase 1-mediated Signaling by the γ134.5 Protein of Herpes Simplex Virus 1," *Journal of Biological Chemistry* 284, no. 2 (2009): 1097–1105, https://doi.org/10.1074/jbc.M805905200.

33. K. D. Smith, J. J. Mezhir, K. Bickenbach, et al., "Activated MEK Suppresses Activation of PKR and Enables Efficient Replication and In Vivo Oncolysis by $\Delta\gamma_1$34.5 Mutants of Herpes Simplex Virus 1," *Journal of Virology* 80, no. 3 (2006): 1110–1120, https://doi.org/10.1128/jvi.80.3.1110-1120.2006.

34. C. A. Alvarez-Breckenridge, J. Yu, R. Price, et al., "NK Cells Impede Glioblastoma Virotherapy TLhrough NKp30 and NKp46 Natural Cytotoxicity Receptors," *Nature Medicine* 18, no. 12 (2012): 1827–1834, https://doi.org/10.1038/nm.3013.

35. T. Lasanen, F. Frejborg, L. M. Lund, et al., "Single Therapeutic Dose of an Antiviral UL29 SIRNA Swarm Diminishes Symptoms and Viral Load of Mice Infected Intranasally With HSV-1," *Smart Medicine* 2, no. 2 (2023): e20230009, https://doi.org/10.1002/SMMD.20230009.

36. K. Kalke, J. Orpana, T. Lasanen, et al., "The In Vitro Replication, Spread, and Oncolytic Potential of Finnish Circulating Strains of Herpes Simplex Virus Type 1," *Viruses* 14, no. 6 (2022): 1290, https://doi.org/10.3390/v14061290.

37. M. Nygårdas, H. Paavilainen, N. Müther, et al., "A Herpes Simplex Virus-Derived Replicative Vector Expressing LIF Limits Experimental Demyelinating Disease and Modulates Autoimmunity," *PLoS One* 8, no. 5 (2013): e64200, https://doi.org/10.1371/journal.pone.0064200.

38. R. K. Mattila, K. Harila, S. M. Kangas, et al., "An Investigation of Herpes Simplex Virus Type 1 Latency in a Novel Mouse Dorsal Root Ganglion Model Suggests a Role for ICP34.5 in Reactivation," *Journal of General Virology* 96, no. 8 (2015): 2304–2313, https://doi.org/10.1099/vir.0.000138.

39. L. Grosche, K. Döhner, A. Düthorn, A. Hickford-Martinez, A. Steinkasserer, and B. Sodeik, "Herpes Simplex Virus Type 1 Propagation, Titration and Single-Step Growth Curves," *Bio-Protocol* 9, no. 23 (2019): e3441, https://doi.org/10.21769/BioProtoc.3441.

40. M. Nygårdas, C. Aspelin, H. Paavilainen, M. Röyttä, M. Waris, and V. Hukkanen, "Treatment of Experimental Autoimmune Encephalomyelitis in SJL/J Mice With a Replicative HSV-1 Vector Expressing Interleukin-5," *Gene Therapy* 18, no. 7 (2011): 646–655, https://doi.org/10.1038/gt.2011.4.

41. A. Sainio, M. Nyman, R. Lund, et al., "Lack of Decorin Expression by Human Bladder Cancer Cells Offers New Tools in the Therapy of Urothelial Malignancies," *PLoS One* 8, no. 10 (2013): e76190, https://doi.org/10.1371/journal.pone.0076190.

42. M. Lagunoff and B. Roizman, "Expression of a Herpes Simplex Virus 1 Open Reading Frame Antisense to the gamma(1)34.5 Gene and Transcribed by an RNA 3' Coterminal With the Unspliced Latency-Associated Transcript," *Journal of Virology* 68, no. 9 (1994): 6021–6028, https://doi.org/10.1128/JVI.68.9.6021-6028.1994.

43. I. Kari, S. Syrjänen, B. Johansson, et al., "Antisense RNA Directed to the Human Papillomavirus Type 16 E7 Mrna From Herpes Simplex Virus Type 1 Derived Vectors Is Expressed in Caski Cells and Down-regulates E7 Mrna," *Virology Journal* 4 (2007): 47, https://doi.org/10.1186/1743-422X-4-47.

44. H. H. Salomäki, A. O. Sainio, M. Söderström, S. Pakkanen, J. Laine, and H. T. Järveläinen, "Differential Expression of Decorin by Human Malignant and Benign Vascular Tumors," *Journal of Histochemistry and Cytochemistry: Official Journal of the Histochemistry Society* 56, no. 7 (2008): 639–646, https://doi.org/10.1369/jhc.2008.950287.

45. M. Nygårdas, T. Vuorinen, A. P. Aalto, D. H. Bamford, and V. Hukkanen, "Inhibition of Coxsackievirus B3 and Related Enteroviruses by Antiviral Short Interfering RNA Pools Produced Using φ6 RNA-Dependent Rna Polymerase," *Journal of General Virology* 90, no. Pt 10 (2009): 2468–2473, https://doi.org/10.1099/vir.0.011338-0.

46. E. K. Broberg, M. Nygårdas, A. A. Salmi, and V. Hukkanen, "Low Copy Number Detection of Herpes Simplex Virus Type 1 mRNA and Mouse Th1 Type Cytokine Mrnas by Light Cycler Quantitative Real-Time PCR," *Journal of Virological Methods* 112, no. 1–2 (2003): 53–65, https://doi.org/10.1016/s0166-0934(03)00191-5.

47. J. L. McKnight, T. M. Kristie, and B. Roizman, "Binding of the Virion Protein Mediating Alpha Gene Induction in Herpes Simplex Virus 1-Infected Cells to Its Cis Site Requires Cellular Proteins," *Proceedings of the National Academy of Sciences* 8420 (1987): 7061–7065, https://doi.org/10.1073/pnas.84.20.7061.

48. J. Mäki, H. Paavilainen, S. Grénman, S. Syrjänen, and V. Hukkanen, "Carriage of Herpes Simplex Virus and Human Papillomavirus in Oral Mucosa Is Rare in Young Women: A Long-Term Prospective Follow-Up," *Journal of Clinical Virology* 70 (2015): 58–62, https://doi.org/10.1016/j.jcv.2015.07.006.

49. A. L. McDoniels-Silvers, C. F. Nimri, G. D. Stoner, R. A. Lubet, and M. You, "Differential Gene Expression in Human Lung Adenocarcinomas and Squamous Cell Carcinomas," *Clinical Cancer Research: An Official Journal of the American Association for Cancer Research* 8, no. 4 (2002): 1127–1138.

50. A. Turunen, V. Hukkanen, M. Nygårdas, J. Kulmala, and S. Syrjänen, "The Combined Effects of Irradiation and Herpes Simplex Virus Type 1 Infection on an Immortal Gingival Cell Line," *Virology Journal* 11 (2014): 125, https://doi.org/10.1186/1743-422X-11-125.

Supporting Information

Additional supporting information can be found online in the Supporting Information section.